Hypoxia stimulates SUMOylation-dependent stabilization of KDM5B

Bingluo Zhou (3120102798@zju.edu.cn)
Zhejiang University https://orcid.org/0000-0001-5931-9903

Yiran Zhu
Zhejiang University

Wenxia Xu
Zhejiang University

Qiyin Zhou
Zhejiang University

Linghui Tan
Zhejiang University

Liyuan Zhu
Zhejiang University School of Medicine Sir Run Run Shaw Hospital

Hui Chen
Zhejiang University School of Medicine Sir Run Run Shaw Hospital

Lifeng Feng
Zhejiang University School of Medicine Sir Run Run Shaw Hospital

Tianlun Hou
Wenzhou Medical University

Xian Wang
Zhejiang University School of Medicine Sir Run Run Shaw Hospital

Dingwei Chen
Zhejiang University School of Medicine Sir Run Run Shaw Hospital

Hongchuan Jin
Zhejiang University School of Medicine Sir Run Run Shaw Hospital https://orcid.org/0000-0002-6697-3097

Research Article

Keywords: hypoxia adaption, GC, KDM5B, SUMOylation, PIAS4, ubiquitination

Posted Date: June 17th, 2021

DOI: https://doi.org/10.21203/rs.3.rs-620216/v1

Version of Record: A version of this preprint was published at Frontiers in Cell and Developmental Biology on December 17th, 2021. See the published version at https://doi.org/10.3389/fcell.2021.741736.

Abstract

Background Hypoxia is an important characteristic of the tumor microenvironment. Tumor cells can survive and propagate under the hypoxia stress through activating a series of adaption response. The study on the mechanism of tumor hypoxia adaption is still of urgent significance to find effective therapeutic targets and strategies.

Methods We compared the protein expression of KDM5B in tumor or normal tissues and cell lines by IHC and Western blotting (WB). CCK8 and cell colony formation assay was performed to evaluate the KDM5B caused growth inhibition. The transcriptome analysis, quantitative real-time PCR (qPCR), flow cytometry analysis, chromatin immunoprecipitation (ChIP) were for exploring the downstream mechanism. And the SUMOylation assay and Ni-beads pull-down assay and co-immunoprecipitation (co-IP) were used to illustrate how did post-translation modification (PTM) regulate the KDM5B protein stabilization. Finally, tumor xenograft assay in nude mice verified the findings in vivo.

Results We found that lysine-specific demethylase 5B (KDM5B) was upregulated in gastric cancer (GC) under hypoxia condition. The genetic knockdown or chemical inhibition of KDM5B impaired the growth of GC cell adapted to hypoxia. Inhibition of KDM5B caused significant cell cycle G1/S arrest through the transcription upregulation of cyclin-dependent kinase inhibitor 1 (CDKN1, also known as p21). Interestingly, the upregulation of KDM5B in hypoxia response was associated with the SUMOylation of KDM5B. SUMOylation stabilized KDM5B protein by reducing the competitive modification of ubiquitination. Furthermore, protein inhibitor of activated STAT 4 (PIAS4) was determined as the SUMO E3 ligase which increased the interaction with KDM5B under hypoxia condition. As the result, co-targeting KDM5B significantly improved the anti-tumor efficacy of antiangiogenic therapy in vivo.

Conclusion Taken together, PIAS4 mediated SUMOylation stabilized KDM5B protein through disturbing ubiquitination-dependent proteasomal degradation to overcome hypoxia adaption. Targeting SUMOylation-dependent KDM5B upregulation might be considered when antiangiogenic therapy was applied in cancer treatment.

Background

Cancer ranks as a leading cause of death and an important barrier to increase life expectancy in every country of the world. According to the report recently released by the International Agency for Research on Cancer, GC remains one of the most common causes of cancer death worldwide. Although multidisciplinary treatment has made big progress [1], GC still ranked the fifth for incidence and the fourth for mortality globally [2]. The understanding of the pathogenesis and development mechanism of GC is attracting considerable attention in order to find effective therapeutic and prevention strategies.

Hypoxia is a state of low oxygen tension which is common in numerous solid tumors typically associated with abnormal vasculature [3]. As a result, tumor cells had to undergo adaptive genetic or epigenetic changes resulting into metabolic remodeling, angiogenesis, or invasiveness to overcome multiple

hypoxia-associated challenges [4]. By doing so, tumor cells adapted to hypoxia have a growth advantage and become resistant to chemotherapy or radiotherapy, conferring worse prognosis [5]. More importantly, anti-angiogenesis has been widely explored and applied in the clinical management of various cancers as a new targeted therapy [6-8]. Co-targeting hypoxia adaption would be essential to improve such anti-angiogenesis therapies.

Epigenetic modifications of chromatin including methylation of histone tails play an important role in genome stability, X-chromosome inactivation, imprinting and transcriptional regulation [9]. Histone lysine demethylases which were responsible for histone demethylation have attracted extensive research interests recently [10,11]. Among them, KDM5B has been reported to be relevant in multiple human cancers including GC [12]. However, the regulation and relevance of KDM5B in hypoxia remains largely undefined.

In this study, we found that the SUMO E3 ligase PIAS4 mediated KDM5B SUMOylation under hypoxia to protect it from ubiquitination-dependent proteasomal degradation, which was important for the hypoxia adaption of GC cells. Genetic or chemical inhibition of KDM5B can disrupt hypoxia adaption both in vitro and in vivo. Thus, targeting KDM5B represents a new companion treatment for anti-angiogenesis or other hypoxia-inducing therapeutics.

Materials And Methods

Cell culture and small molecule chemical inhibitors

Nine Human GC cell lines (SGC7901, BGC823, MKN45, AGS, HGC-27, MKN28, MGC803, N87, and MFC), a human normal gastric epithelial cell line (GES-1), and HEK293T were all purchased from Cell Bank of the Typical Culture Preservation Committee, Chinese Academy of Sciences (Shanghai, China). MEF cells from *Pias4+/+ and Pias4-/-* mice were generous gifts from Prof. Shuai Ke (University of California, Los Angeles, Los Angeles, CA, USA) [13]. SGC7901/BGC823-shNC and SGC7901/BGC823-shKDM5B cells were generated via infection of lentiviral vectors containing shRNA (shscramble and shKDM5B) and puromycin selection. The cells were cultured according to the culture conditions previously reported [14].

The chemicals used in this study include: JIB04 (S7281, Selleck), 2-D08 (S8696, Selleck), TAK-981 (S8829, Selleck), ADOX (S8608, Selleck), MS049 (S8147, Selleck), AMI-1 (S7884, Selleck), EX527 (S1541, Selleck), TSA (S1045, Selleck), A485 (S8740, Selleck), C646 (S7152, Selleck), Okadaic acid (OA) (S1786, Beyotime), MG132 (474790, Calbiochem, USA), CHX (C7698, Sigma-Aldrich), and NEM (Sigma-Aldrich, E3876).

The antibodies used were listed as follows: anti-KDM5B (Abcam ab181089, for WB), anti-KDM5B (Abcam ab211366, for IHC), anti-β-Actin (Abclonal ac026), anti-PIAS4 (CST 4392s), anti-Flag-tag (Sigma-Aldrich F1804-1), anti-HA-tag (earthox, E022010), anti-V5-tag (Invitrogen 46-0705), anti-p-RB (CST 8516S), anti-p21 (CST 2946S), anti-Cyclin E (CST 20808), anti-UB (Santa cruz sc-8071), and anti-His (Proteintech 66005-1-ig).

SiRNA and plasmids

Small interfering RNA (siRNA) targeting KDM5B, PIAS1, PIAS2, PIAS3, PIAS4 were synthesized by Genepharma Company (Shanghai, China). The sequences of these siRNAs were listed in Additional file: Table. S1. The siRNAs were transfected into cells seeded overnight using Lipofectamine RNAiMAX transfection reagent (Invitrogen, USA) according to the manufacturer's instruction.

The plasmid of Flag-KDM5B was constructed by GeneChem Company (Shanghai, China). The plasmid of PIAS4-HA tag was purchased from Sino Biologic Inc (Beijing, China). SUMO1/2/3 ORFs with V5 or His tag were cloned to pCMV3 vector. Quick Change Site-Directed Mutagenesis Kit (Agilent, USA) was used to generate PIAS4 mutants and non-conjugation SUMO mutants SUMO1/2/3ΔGG. The primers used were shown in Additional file: Table S2. Plasmids were transfected into cells seeded overnight with X-tremeGENE HP DNA Transfection Reagent (Roche, Basel, Switzer-land) as the instruction provided. After transfection for 48 to 72 hours, cells were used for RNA or protein extraction and other assays.

RNA isolation and quantitative real-time PCR (qPCR)

Total RNA was extracted by Trizol reagent (Invitrogen, USA). The concentration of total RNA was quantified by NanoDrop 2000. And 2 μg of total RNA was taken for reverse transcription using High-Capacity cDNA Reverse Transcription Kit (Applied Biosystems, USA). The relative expression level of each mRNA was determined by qPCR with the SYBR Green Master reagents (Applied Biosystems, USA). The primers were displayed in Additional file: Table 3.

Western blotting (WB)

Proteins from cells and tissues were extracted by RIPA lysis buffer (Beyotime, Beijing, China) and quantified by BCA Protein Assay Kit (Beyotime, Beijing, China). Lysates with 20-30 μg protein were loaded to SDS-PAGE gel for separating proteins of different molecular weights and transferred to the PVDF membranes. the membranes were blocked with 5% skimmed milk dissolved inTBS for 1h. Subsequently, membranes were incubated with primary antibody overnight in 4 ℃, followed by incubation with secondary antibody labeled with peroxidase (Jackson ImmunoResearch Inc., PA, USA) for 1h in room temperature. The WB bands were visualized with ECL substrate.

Immunoprecipitation

Cells were washed with ice PBS twice and lysed on ice in 20 mM Triton buffer containing 50mM Tris-HCl (PH 7.4), 150 mM NaCl, 1% Triton-X-100 and protease inhibitor cocktail. The lysates were incubated with primary antibodies overnight in 4℃. The next day, protein A/G sepharose beads were added into the lysates. After rotation in 4℃ for at least 3 hours, the beads were washed with lysis buffer for 5 times. The bound proteins were then eluted and detected by western blotting as described above.

Chromatin immunoprecipitation (ChIP)

ChIP analysis was implemented with the SimpleChIP™ Enzymatic Chromatin IP Kit (CST, USA) as the protocol provided by the kit, using the antibody anti-Tri-methylation H3K4 (CST, 1: 100) and negative control anti-IgG. The primers used for the PCR analysis of precipitated DNA were shown in Additional file: Table S3.

Immunohistochemistry (IHC)

The tumors from the mice with the indicated treatment and tissues from GC patients in the tissue microarray as indicated were fixed with 4% paraformaldehyde. For IHC staining, the tissues were incubated with diluted primary antibodies at 4 °C overnight as described in the instruction manual. And then they were incubated with biotinylated secondary antibody, followed with 3,3'-diaminobenzidine (DAB) and hematoxylin staining the next day. The results were observed and analyzed by a professional pathologist. Digital images of 5 random regions were taken for per tissue section. And the H-score was applied to quantify the analysis result which was calculated using the following formula: H-score = 0 * (%cells with zero intensity) + 1 * (%cells with 1+ intensity) + 2 * (%cells with 2+ intensity) + 3 * (%cells with 3+ intensity).

Human gastric tissue specimens

The GC and corresponding normal tissues for IHC and WB were all collected from Sir Run Run Shaw hospital (Hangzhou China), informed consent was obtained from all individuals.

Ni-beads pull-down assay

To determine the ubiquitination of KDM5B, HEK293T cells were co-transfected with plasmids as indicated including His-HA-UB or His-SUMO1/2/3 for 42h. Subsequently, the cells were treated with MG132 (20 μM) for 6h and then lysed in the solution as previously reported [15]. Then, KDM5B-UB or KDM5B-SUMO was pulled-down by the Ni-beads and washed. The proteins were eluted and analyzed by western blotting as described above.

SUMOylation Assay

To detect the SUMOylation of KDM5B, the protocol as reported [16] before was introduced. In brief, HEK293T cells were co-transfected with plasmids as indicted for 48h. The cells were lysed with 2X lysis buffer (1X PBS, 2% (wt/vol) SDS, 10mM EDTA, 10mM EGTA, 10mM NEM) at room temperature followed with Sonication twice with a microtip (25 pulses with 30 duty cycles and output control of 3). The samples were added 50 μl DTT solution (50mM final concentration) and boiled at 97 ℃ for 10 min. 1/10 lysate was obtained as input before diluting the lysate with 1% Triton buffer with NEM as described in the Immunoprecipitation assay (1:10 dilution). After centrifuging at 16000g for 15min, the supernatant was incubated with Flag antibody by rotating at 4 ℃ overnight and later with the same steps as described in the Immunoprecipitation assay.

Plate colon formation assay

Cells as indicated were seeded into 6-well plates at a concentration of 500 cells per well. The cells were subsequently incubated with the treatments as indicted for 10 days. The monoclonal colonies with more than 50 cells were counted and qualified with the crystal violet staining.

Flow cytometry analysis

The cell cycle was determined using the cell cycle staining kit (Multi Sciences, Hangzhou, China), using Propidium iodide (PI) staining. And the apoptosis was determined by the apoptosis staining kit (Multi Sciences, Hangzhou, China) with PI and Annexin-V FITC. The cell suspensions were analyzed by flowcytometry.

In situ proximity ligation assay (PLA)

PLA was performed using the Duolink kit (Sigma) following the manufacturer's instructions. HEK293T were co-transfected with Flag-KDM5B and HA-PIAS4, primary mouse anti-Flag and primary rabbit anti-PIAS4 were applied to the fixed and permeabilized cells for 4 hours at 4 °C. After washing, PLUS and MINUS PLA probes provided by the kit were incubated with the primary antibodies for 1h in humidity chamber at 37°C. Then, wash away the probed, and incubated the cells in ligation and amplification buffer in the kit sequentially in humidity chamber at 37°C. The slide was then mounted with DAPI and the coverslip sealed. The PLA signals were visualized as red fluorescent spots.

Tumor xenograft assay

Five-week-old female BALB/c nude mice from the Center of Experimentation of Zhejiang University were fed and housed. And the procedures were performed in compliance with NIH Guide for the Care and Use of Laboratory Animals. Tumors were established by subcutaneous injection (5×10^6 MFC cells in 0.1 ml saline) into the flanks of the mice. When the tumors exceeded 100–150 mm^3 in size, the mice were evenly distributed into groups as indicated (n=6/group) with treatment of JIB04 (55 mg/kg body weight; i.g, every 2 days), 2-D08 (5 mg/kg body weight; i.p, every 2days), Endostar (8 mg/kg body weight; i.p, every 2 days) or equal volume of solvent as indicated at the same time respectively. The volume of tumors and body weight were measured every 2 days. The mice were sacrificed when the tumors size reached approximately 1500 mm^3. And the volume of tumors was calculated using the formula: (length×width2)/2.

Statistical Analysis

All data were presented as mean ± SD and as all experiments were performed at least three times independently. Statistical approach used in every experiment to compare the differences between groups were indicated in Fig. legends. $P<0.05$ was respected as statistically.

Results

KDM5B was upregulated in GC

To investigate the involvement of KDM5B in GC, we examined KDM5B expression by immunohistochemical staining in tissue microarrays (TMAs) containing collected tumor tissue samples and the matched normal adjacent tissues from 77 GC patients. As shown in Fig. 1a and b, the expression of KDM5B was much higher in cancer tissues than normal tissues. Next, we determined KDM5B protein expression by Western blotting. In consistence with immunohistochemical staining results, KDM5B expression was upregulated in tumor tissues and GC cell lines compared to matched normal tissues and human normal gastric epithelial cell line GES-1 (Fig. 1c, d). Importantly, both plate colony formation and CCK8 assay verified that KDM5B knockdown significantly inhibited cell proliferation of GC cells (Fig. 1e-g, Additional file: Fig. S1a, b). Similarly, the chemical inhibitor JIB04, a selective JmjC histone demethylase inhibitor, could significantly inhibit the proliferation of GC cells (Fig. 1h-i, and Additional file: Fig. S1c-e). Taken together, these results suggest that KDM5B is upregulated to stimulate cell proliferation in GC.

KDM5B inhibition upregulated p21 expression

To further explore the underlying mechanism of growth inhibition induced by KDM5B inhibition, we performed RNA sequencing on JIB-04-treated GC cells. The cluster analysis showed that the gene expression profile was significantly changed after JIB-04 treatment (Fig. 2a). Kyoto Encyclopedia of Genes and Genomes (KEGG) pathway analysis indicated that DEGs (differential expressed genes) were enriched in ‘cell cycle’ and ‘apoptosis’ pathways (Fig. 2b). Therefore, Flow cytometry was used to detect cell cycle distribution and cell apoptosis before and after KDM5B inhibition. Interestingly, cell cycle arrest at G1 phase and subsequent cell apoptosis was greatly induced by JIB04 (Fig. 2c, Additional file: Fig. S2a-d). As a result, we focused on 18 differentially expressed genes related to cell cycle regulation (Fig. 2d). After verification by qPCR, p21 turned out to be the most significantly upregulated gene (Fig. 2e). It is well known that KDM5B could reduce H3K4 tri-methylation to repress gene transcription. As expected, chromatin immunoprecipitation (ChIP) analysis indeed revealed increased tri-methylation H3K4 occupancy at the site after JIB04 treatment that p21 promoter was bounded to tri-methylation H3K4 (Fig. 2f). Consistently, protein p21 was significantly up-regulated after KDM5B inhibition by JIB04 while the levels of phosphorylated RB, and other G1 phase-related regulators such as cyclin E and CDK6 were significantly decreased (Fig. 2g). Once p21 expression was knocked down, the effect of KDM5B inhibition on G1 arrest was partly reversed (Fig. 2h). Overall, these results indicate that KDM5B promotes H3K4 demethylation to repress p21 transcription, thus resulting in G1 arrest.

KDM5B protein was upregulated to facilitate hypoxia adaption

Cancer cells undergo a variety of biological responses enable cellular survival under various stresses such as hypoxia. Interestingly, the expression of KDM5B signature which was defined by genes significantly down-regulated after JIB04 treatment correlated positively with the expression of the previously reported hypoxia signature [17], based on TCGA data analysis (Fig. 3a). Indeed, KDM5B protein expression was increased significantly as early as 2h after hypoxia in both SGC7901 (Fig. 3b) and BGC823 (Fig. 3c) cells but not the non-tumor gastric epithelial GES-1 cells (Fig. 3d). Furthermore, both the colony formation (Fig. 3e, f) and viability (Fig. 3g) of GC cells were impaired significantly under hypoxia

condition once KDM5B expression was knocked down. Taken together, GC cells upregulates KDM5B protein expression to adapt hypoxia.

Hypoxia induced SUMO3-dependent SUMOylation and subsequent stabilization of KDM5B

Much to our surprise, KDM5B mRNA expression was not altered as KDM5B protein (Fig. 4a, b). Meanwhile, the half-life of KDM5B protein was obviously extended under 1%O_2 treatment (Fig. 4c, Additional file: Fig. S4a). Therefore, hypoxia seems to stabilize KDM5B protein. Given that the post-translational modification (PTM) has been regarded as a key factor affecting protein stability [18], we screened the effect of common PTMs including SUMOylation, acetylation, methylation and phosphorylation on KDM5B protein stability with corresponding inhibitors (Additional file: Fig. S4b). Only 2-D08 which was the inhibitor of SUMOylation [19] could remarkably decrease KDM5B protein expression, implicating the involvement of SUMOylation on the regulation of KDM5B protein stability. In fact, the increase of KDM5B protein expression under hypoxia was compromised by 2-D08 dose-dependently (Fig. 4d). And similar effect was achieved with another SUMOylation inhibitor TAK-981 [20] (Fig. 4e). What's more, SUMOylation inhibition significantly shortened the half-life of KDM5B protein in both SGC7901 and BGC823 cells under hypoxia (Fig. 4f, Additional file: Fig. S4c). These results indicated that SUMOylation might directly or indirectly affect the stability of KDM5B protein.

Indeed, KDM5B protein could be modified by SUMO1/2/3 but not non-conjugation SUMO mutants (SUMO1/2/3ΔGG) [21] (Additional file: Fig. S4d). However, only the SUMO3-mediated SUMOylation was enhanced significantly by hypoxia (Fig. 4g), and 2-D08 dramatically diminished SUMO3-mediated SUMOylation induced by hypoxia (Fig. 4h). Collectively, SUMO3-mediated SUMOylation of KDM5B was enhanced to under hypoxia stress and increased the stability of KDM5B protein.

PIAS4 was the SUMO E3 ligase for hypoxia-induced KDM5B SUMOylation

Next, we sought to determine which SUMO E3 ligase might be response for the SUMOylation of KDM5B protein. Since the PIAS family is the most well-known SUMO E3 ligase family [22], we performed a siRNA-based screen for the effect of PIAS family SUMO E3 ligases on KDM5B expression in hypoxic cells. As shown, KDM5B protein expression was reduced in GC cells with PIAS4 knocking down (Fig. 5a, Additional file: Fig. S5b). Similarly, KDM5B protein expression level was much lower in *Pias4*-/- MEF cells than in *Pias4*+/+ MEF cells [13] (Additional file: Fig. S5c). Meanwhile, the half-life of KDM5B protein was shortened in GC cells with PIAS4 knock-down (Fig. 5b, Additional file: Fig. S5d). Furthermore, the interaction of PIAS4 with KDM5B could be confirmed by either co-IP assay (Fig. 5c, d) or PLA assay (Additional file: Fig. S5e), which also implicated their co-localization in the nucleus consistent with the distribution of KDM5B and PIAS4 in nuclear fraction (Additional file: Fig. S5f). In addition, KDM5B SUMOylation could be enhanced only by wild-type PIAS4 but not its mutants lacking E3 ligase activity (Fig. 5e, f). More importantly, the interaction of KDM5B with PIAS4 and its SUMOylation was enhanced by hypoxia (Fig. 5g-h). Collectively, PIAS4 was the E3 ligase responsible for hypoxia-induced SUMOylation of KDM5B.

PIAS4-mediated KDM5B SUMOylation prevented it from ubiquitination-dependent proteasomal degradation

As we previously reported, KDM5B protein turnover can be regulated by the ubiquitin-proteasome system [23]. More interestingly, the sites of KDM5B predicted by online databases to be most-likely modified by SUMOylation and ubiquitination were K242 and K278 (Additional file: Fig. S6a, b), Furthermore, the SUMOylation sites were also verified by Ivo A. Hendriks et al [24], thus indicating a potential influence of SUMOylation on ubiquitination-dependent degradation of KDM5B. Indeed, the proteasome inhibitor MG132 notably reversed the decrease of KDM5B protein expression caused by function loss of PIAS4 in both GC cells and MFE cells (Fig. 6a-c). While KDM5B underwent ubiquitination-dependent degradation in SGC7901 cells under normoxia (Fig. 6d), hypoxia significantly reduced the ubiquitination of KDM5B to prevent it subsequent degradation (Fig. 6e), which was reversed by SUMOylation inhibitor 2-D08 (Fig. 6f). In accordance with that, the ubiquitination of KDM5B was increased after PIAS4 knockdown (Fig. 6g). Taken together, these results suggested that PIAS4 SUMOylated KDM5B to prevent it from ubiquitination-dependent degradation under hypoxia.

PIAS4 upregulated KDM5B to promote hypoxia adaption

It has been reported that PIAS4 played critical roles in regulating the function or expression of proteins important to hypoxia response including VHL, the ubiquitination E3 ligase for HIF1α [25,26]. Thus, we speculated that PIAS4 might upregulate KDM5B to enable the adaption of GC cells to hypoxia. As expected, knocking down PIAS4 inhibited the viability (Fig. 7a-d) and colony formation (Fig. 7e-h) as well as induced apoptosis (Fig. 7i) of GC cells under hypoxia, which could be partially restored by the overexpression of KDM5B.

Targeting KDM5B to overcome hypoxia adaption in vivo

Given the dependence of hypoxia adaption on KDM5B upregulation, targeting KDM5B might be an ideal strategy to overcome hypoxia adaption of cancer cells under anti-vascular treatment. Indeed, tumor growth in nude mice was only moderately attenuated after the treatment of Endostar, recombinant human endostatin used for the clinical treatment of patients with various cancers including GC [27,28]. However, the addition of JIB04 or 2-D08 significantly improved the Endostar-induced inhibitory effect on tumor growth in vivo (Fig. 8a-d). In line with the finding in cells that KDM5B inhibition impaired GC cells to adapt hypoxia as indicated above.

Discussion

In this study, we reported that PIAS4-mediated SUMOylation protected KDM5B from ubiquitination-dependent proteasomal degradation to enable hypoxia adaption in gastric cancer (Fig. 8e). KDM5B was upregulated in gastric cancer and further stabilized under hypoxia through SUMOylation-mediated inhibition of its ubiquitination-dependent proteasomal degradation. This upregulation of KDM5B enabled the survival of gastric cancer cells under hypoxia through inhibiting the transcription of CDKN1A (p21).

It has been well-known that hypoxia-inducible Factor-1α (HIF1α) is critical in hypoxia response. Recently, additional sigailing pathways such as mTOR and UPR (unfolded protein response) pathway has been revealed to play important roles in response to hypoxa [29]. Mammmalian cells contain a type of enzymes called 2-oxoglutarate-dependent dioxygenases (2-OGDDs) which take oxygen as the substrates for enzymatic reactions. Many 2-OGDDs act on remodeling chromatin structure as metrhylation erasers such as DNA demethylases TETs and numerous histone lysine demethylases, thus linking oxygen concentration with epigenetic reprogramming [30,31]. Likewise, thypoxia caused DNA hypermethylation in cancer cells by reducing TET activity [32]. Furthermore, lysine methylation of HIF-1α protein regulated by histone demethylase LSD1 influenced its stability of nuclear HIF-1α independent of its proline hydroxylation [33,34]. It would be valuable to undertand cellular response to hypoxia and design effective strategies for hypoxia-targeting therapies such as anti-angiogenesis approaches, by clarifying the relevance and regulation of more signaling pathways associated with hypoxia response. In this study, we found that SUMOylation-dependent stablization of KDM5B is important to confer hypoxia adaption in gastric cancer. Lysine SUMOylation is a reversible post-translational modification which efficiently regulate the localization and function of various proteins [35]. For instance, HIF-1α wasSUMOylated by Cbx4 to transactivate the transcription ofVEGF [36], which could be reversed by RSUME and SENP1 dependent-deSUMOylation[37,38]. Interestingly, PIAS4 mediated SUMOylation of VHL blocked its ubiquitination-dependent degradation, thus upregulating HIF-1α protein expression [25,26]. Here we found KDM5B as another downstream targets of PIAS4 in the hypoxia response. The growth inhibition induced by PIAS4 inhibition could be partialy rescued by the overexpression of KDM5B (Figure 7), highlighting the importance of KDM5B in the hypoxia response. Although KDM5B was well-known to predominatly affect gene expression through demethylating histones, KDM5B and other family members may translocated in the cytoplasm to demethylate non-histone proteins. Whether such functions might be relevant to hypoxia adaption remains to be further explored.

Nevertheless, the crosstalk between SUMOylation and ubiquitination was extensively explored recently. Same proteins can be conjugated to SUMO and ubiquitin for antagonistic, synergistic or other outcomes, demonstrating the complexity of the cellular signalling networks. For example, the dual modification at Lys^{21} of IκBα led to oppsite results to its stabilization and sebsquent NF-κB activation [39]. In contrast, these two modifications formed a cooperative relationship in a sequential manner under some situations. In response to DNA damage, hybrid SUMO-ubiquitin chains can be synthesized by RNF4, a SUMO-targeted ubiquitin E3 ligase, thus recruiting RAP80 and BRCA1 to sites of DNA damage[40]. In our study, the SUMOylation and ubiquitination of KDM5B seems to be exclusive for the stalization of KDM5B protein. However, the underlying mechanisms including the identification of the ubiquitin E3 ligase warrants further investigations.

Despite the important role of angiogenesis in GC, clinical trials of anti-vascular therapy in GC have not yielded encouraging results so far [41]. Therefore, targeting hypoxia adaption could be necessary to improve the clinical efficacy of anti-vascular therapy in GC. Our study indicated that KDM5B was a key regulatory factor in hypoxia adaption. Targeted inhibition of KDM5B might be considered in combination

of anti-vascular therapy in GC. As KDM5B was upregulated to play an oncogenic role in multiple cancers, many chemical inhibitors of KDM5B have been extensively evaluated for their potential in targetd therapy of huamn cancers [42,43]. The combination of these inhibitors with anti-vascular therapy could be taken into consideration while designing upcoming clinical trials.

Conclusions

In conclusion, PIAS4 mediated SUMOylation stabilized KDM5B protein through disturbing ubiquitination-dependent proteasomal degradation to overcome hypoxia adaption. Targeting SUMOylation-dependent KDM5B upregulation might be considered when anti-angiogenic therapy was applied in cancer treatment.

Abbreviations

KDM5B: lysine-specific demethylase 5B

GC: gastric cancer

CDKN1: cyclin-dependent kinase inhibitor 1

SUMO: Small Ubiquitin-related Modifier

PIAS4: protein inhibitor of activated STAT 4

qPCR: quantitative real-time PCR

IHC: Immunohistochemistry

WB: Western blotting

ChIP: chromatin immunoprecipitation

co-IP: co-immunoprecipitation

PLA: In situ proximity ligation assay

TMA: tissue microarray

KEGG: Kyoto Encyclopedia of Genes and Genomes

DEG: differential expressed gene

TCGA: The Cancer Genome Atlas

PTM: post-translation modification

Declarations

Ethics approval and consent to participate

The research was approved by the Ethics Committee of Sir Run Run Shaw Hospital, Zhejiang University School of Medicine. Animal care and experiments were conducted in compliance with Institutional Animal Care and Use Committee and NIH guidelines.

Consent for publication

If this article is accepted, we will agree to publish it and transfer the copyright to academic journals and your publishing company.

Availability of data and materials

The datasets used and analysed during the current study are available from the corresponding author on reasonable request.

Competing interests

The authors declare no competing interests.

Funding

This work was supported by Nature Science foundation of Zhejiang (Y19H160258, LD21H160001) and high level health innovative talents program in Zhejiang.

Author's contributions

HCJ, BLZ, DWC, XW, WXX, TLH, LFF designed the study; HCJ, BLZ, DWC, YRZ, LHT, LYZ analyzed the data and wrote the manuscript; BLZ, YRZ, HC, QYZ, LYZ, WXX performed the experiments. All authors read and approved the final manuscript

Acknowledgements

Not applicable

Author information

Affiliations

Laboratory of Cancer Biology, Key Lab of Biotherapy in Zhejiang Province, Cancer Center of Zhejiang University, Sir Run Run Shaw hospital, School of Medicine, Zhejiang University, Hangzhou, Zhejiang, China

Bingluo Zhou, Yiran Zhu, Wenxia Xu, Linghui Tan, Liyuan Zhu, Hongchuan Jin

Department of Medical Oncology, Sir Run Run Shaw hospital, School of Medicine, Zhejiang University, Hangzhou, Zhejiang, China

Qiyin Zhou, Xian Wang

Department of Pathology, Sir Run Run Shaw hospital, School of Medicine, Zhejiang University, Hangzhou, Zhejiang, China

Hui Chen

Department of Clinical Medicine, Wenzhou Medical University, Wenzhou, Zhejiang, China

Tianlun Hou

Department of General Surgery, Sir Run Run Shaw hospital, School of Medicine, Zhejiang University, Hangzhou, Zhejiang, China

Dingwei Chen

References

1 Joshi, S. S. & Badgwell, B. D. Current treatment and recent progress in gastric cancer. *CA Cancer J Clin* **71**, 264-279, doi:10.3322/caac.21657 (2021).

2 Sung, H. *et al.* Global Cancer Statistics 2020: GLOBOCAN Estimates of Incidence and Mortality Worldwide for 36 Cancers in 185 Countries. *CA Cancer J Clin* **71**, 209-249, doi:10.3322/caac.21660 (2021).

3 Sharma, A. *et al.* Hypoxia-targeted drug delivery. *Chem Soc Rev* **48**, 771-813, doi:10.1039/c8cs00304a (2019).

4 Patel, A. & Sant, S. Hypoxic tumor microenvironment: Opportunities to develop targeted therapies. *Biotechnol Adv* **34**, 803-812, doi:10.1016/j.biotechadv.2016.04.005 (2016).

5 Hammond, E. M. & Giaccia, A. J. Hypoxia-inducible factor-1 and p53: friends, acquaintances, or strangers? *Clinical cancer research : an official journal of the American Association for Cancer Research* **12**, 5007-5009, doi:10.1158/1078-0432.CCR-06-0613 (2006).

6 Ohtsu, A. *et al.* Bevacizumab in combination with chemotherapy as first-line therapy in advanced gastric cancer: a randomized, double-blind, placebo-controlled phase III study. *J Clin Oncol* **29**, 3968-3976, doi:10.1200/JCO.2011.36.2236 (2011).

7 Yoon, H. H. *et al.* Ramucirumab combined with FOLFOX as front-line therapy for advanced esophageal, gastroesophageal junction, or gastric adenocarcinoma: a randomized, double-blind, multicenter Phase II trial. *Ann Oncol* **27**, 2196-2203, doi:10.1093/annonc/mdw423 (2016).

8 Fuchs, C. S. *et al.* Ramucirumab monotherapy for previously treated advanced gastric or gastro-oesophageal junction adenocarcinoma (REGARD): an international, randomised, multicentre, placebo-controlled, phase 3 trial. *Lancet* **383**, 31-39, doi:10.1016/S0140-6736(13)61719-5 (2014).

9 Nowak, R. P. *et al.* Advances and challenges in understanding histone demethylase biology. *Curr Opin Chem Biol* **33**, 151-159, doi:10.1016/j.cbpa.2016.06.021 (2016).

10 Hojfeldt, J. W., Agger, K. & Helin, K. Histone lysine demethylases as targets for anticancer therapy. *Nat Rev Drug Discov* **12**, 917-930, doi:10.1038/nrd4154 (2013).

11 Kooistra, S. M. & Helin, K. Molecular mechanisms and potential functions of histone demethylases. *Nat Rev Mol Cell Biol* **13**, 297-311, doi:10.1038/nrm3327 (2012).

12 Xhabija, B. & Kidder, B. L. KDM5B is a master regulator of the H3K4-methylome in stem cells, development and cancer. *Seminars in cancer biology* **57**, 79-85, doi:10.1016/j.semcancer.2018.11.001 (2019).

13 Yu, X. *et al.* Chromatin remodeling: demethylating H3K4me3 of type I IFNs gene by Rbp2 through interacting with Piasy for transcriptional attenuation. *FASEB journal : official publication of the Federation of American Societies for Experimental Biology* **32**, 552-567, doi:10.1096/fj.201700088RR (2018).

14 Xu, J. *et al.* Metabolic enzyme PDK3 forms a positive feedback loop with transcription factor HSF1 to drive chemoresistance. *Theranostics* **9**, 2999-3013, doi:10.7150/thno.31301 (2019).

15 Zhou, Q. *et al.* Inhibiting neddylation modification alters mitochondrial morphology and reprograms energy metabolism in cancer cells. *JCI Insight* **4**, doi:10.1172/jci.insight.121582 (2019).

16 Barysch, S. V., Dittner, C., Flotho, A., Becker, J. & Melchior, F. Identification and analysis of endogenous SUMO1 and SUMO2/3 targets in mammalian cells and tissues using monoclonal antibodies. *Nat Protoc* **9**, 896-909, doi:10.1038/nprot.2014.053 (2014).

17 Harris, A. L. Hypoxia–a key regulatory factor in tumour growth. *Nat Rev Cancer* **2**, 38-47, doi:10.1038/nrc704 (2002).

18 Buuh, Z. Y., Lyu, Z. & Wang, R. E. Interrogating the Roles of Post-Translational Modifications of Non-Histone Proteins. *J Med Chem* **61**, 3239-3252, doi:10.1021/acs.jmedchem.6b01817 (2018).

19 Kim, Y. S., Keyser, S. G. & Schneekloth, J. S., Jr. Synthesis of 2',3',4'-trihydroxyflavone (2-D08), an inhibitor of protein sumoylation. *Bioorg Med Chem Lett* **24**, 1094-1097, doi:10.1016/j.bmcl.2014.01.010 (2014).

20 Langston, S. P. *et al.* Discovery of TAK-981, a First-in-Class Inhibitor of SUMO-Activating Enzyme for the Treatment of Cancer. *J Med Chem* **64**, 2501-2520, doi:10.1021/acs.jmedchem.0c01491 (2021).

21 Yuan, H. *et al.* Small ubiquitin-related modifier paralogs are indispensable but functionally redundant during early development of zebrafish. *Cell Res* **20**, 185-196, doi:10.1038/cr.2009.101 (2010).

22 Rabellino, A., Andreani, C. & Scaglioni, P. P. The Role of PIAS SUMO E3-Ligases in Cancer. *Cancer research* **77**, 1542-1547, doi:10.1158/0008-5472.CAN-16-2958 (2017).

23 Xu, W. *et al.* KDM5B demethylates H3K4 to recruit XRCC1 and promote chemoresistance. *International journal of biological sciences* **14**, 1122-1132, doi:10.7150/ijbs.25881 (2018).

24 Hendriks, I. A. *et al.* Site-specific characterization of endogenous SUMOylation across species and organs. *Nature communications* **9**, 2456, doi:10.1038/s41467-018-04957-4 (2018).

25 Cai, Q., Verma, S. C., Kumar, P., Ma, M. & Robertson, E. S. Hypoxia inactivates the VHL tumor suppressor through PIASy-mediated SUMO modification. *PloS one* **5**, e9720, doi:10.1371/journal.pone.0009720 (2010).

26 Chien, W. *et al.* PIAS4 is an activator of hypoxia signalling via VHL suppression during growth of pancreatic cancer cells. *Br J Cancer* **109**, 1795-1804, doi:10.1038/bjc.2013.531 (2013).

27 Xu, R. *et al.* Results of a randomized and controlled clinical trial evaluating the efficacy and safety of combination therapy with Endostar and S-1 combined with oxaliplatin in advanced gastric cancer. *Onco Targets Ther* **6**, 925-929, doi:10.2147/OTT.S46487 (2013).

28 Eder, J. P., Jr. *et al.* Phase I clinical trial of recombinant human endostatin administered as a short intravenous infusion repeated daily. *J Clin Oncol* **20**, 3772-3784, doi:10.1200/JCO.2002.02.082 (2002).

29 Wouters, B. G. & Koritzinsky, M. Hypoxia signalling through mTOR and the unfolded protein response in cancer. *Nat Rev Cancer* **8**, 851-864, doi:10.1038/nrc2501 (2008).

30 Batie, M. *et al.* Hypoxia induces rapid changes to histone methylation and reprograms chromatin. *Science* **363**, 1222-1226, doi:10.1126/science.aau5870 (2019).

31 Chakraborty, A. A. *et al.* Histone demethylase KDM6A directly senses oxygen to control chromatin and cell fate. *Science* **363**, 1217-1222, doi:10.1126/science.aaw1026 (2019).

32 Thienpont, B. *et al.* Tumour hypoxia causes DNA hypermethylation by reducing TET activity. *Nature* **537**, 63-68, doi:10.1038/nature19081 (2016).

33 Kim, Y. *et al.* Methylation-dependent regulation of HIF-1alpha stability restricts retinal and tumour angiogenesis. *Nature communications* **7**, 10347, doi:10.1038/ncomms10347 (2016).

34 Lee, J. Y. *et al.* LSD1 demethylates HIF1alpha to inhibit hydroxylation and ubiquitin-mediated degradation in tumor angiogenesis. *Oncogene* **36**, 5512-5521, doi:10.1038/onc.2017.158 (2017).

35 Wilson, V. G. Introduction to Sumoylation. *Adv Exp Med Biol* **963**, 1-12, doi:10.1007/978-3-319-50044-7_1 (2017).

36 Li, J. *et al.* Cbx4 governs HIF-1alpha to potentiate angiogenesis of hepatocellular carcinoma by its SUMO E3 ligase activity. *Cancer cell* **25**, 118-131, doi:10.1016/j.ccr.2013.12.008 (2014).

37 Carbia-Nagashima, A. *et al.* RSUME, a small RWD-containing protein, enhances SUMO conjugation and stabilizes HIF-1alpha during hypoxia. *Cell* **131**, 309-323, doi:10.1016/j.cell.2007.07.044 (2007).

38 Cheng, J., Kang, X., Zhang, S. & Yeh, E. T. SUMO-specific protease 1 is essential for stabilization of HIF1alpha during hypoxia. *Cell* **131**, 584-595, doi:10.1016/j.cell.2007.08.045 (2007).

39 Desterro, J. M., Rodriguez, M. S. & Hay, R. T. SUMO-1 modification of IkappaBalpha inhibits NF-kappaB activation. *Molecular cell* **2**, 233-239, doi:10.1016/s1097-2765(00)80133-1 (1998).

40 Guzzo, C. M. *et al.* RNF4-dependent hybrid SUMO-ubiquitin chains are signals for RAP80 and thereby mediate the recruitment of BRCA1 to sites of DNA damage. *Sci Signal* **5**, ra88, doi:10.1126/scisignal.2003485 (2012).

41 Raimondi, A. *et al.* Genomic markers of resistance to targeted treatments in gastric cancer: potential new treatment strategies. *Pharmacogenomics* **19**, 1047-1068, doi:10.2217/pgs-2018-0077 (2018).

42 Fu, Y. D. *et al.* Targeting histone demethylase KDM5B for cancer treatment. *Eur J Med Chem* **208**, 112760, doi:10.1016/j.ejmech.2020.112760 (2020).

43 Zheng, Y. C. *et al.* Lysine demethylase 5B (KDM5B): A potential anti-cancer drug target. *Eur J Med Chem* **161**, 131-140, doi:10.1016/j.ejmech.2018.10.040 (2019).

44 Sachdev, S. *et al.* PIASy, a nuclear matrix-associated SUMO E3 ligase, represses LEF1 activity by sequestration into nuclear bodies. *Genes & development* **15**, 3088-3103, doi:10.1101/gad.944801 (2001).

45 Gross, M., Yang, R., Top, I., Gasper, C. & Shuai, K. PIASy-mediated repression of the androgen receptor is independent of sumoylation. *Oncogene* **23**, 3059-3066, doi:10.1038/sj.onc.1207443 (2004).

oi:10.1200/JCO.2011.36.2236.

- Yoon HH, et al. Ramucirumab combined with FOLFOX as front-line therapy for advanced esophageal, gastroesophageal junction, or gastric adenocarcinoma: a randomized, double-blind, multicenter Phase II trial. Ann Oncol. 2016;27:2196–203. doi:10.1093/annonc/mdw423.
- Fuchs CS, et al. Ramucirumab monotherapy for previously treated advanced gastric or gastro-oesophageal junction adenocarcinoma (REGARD): an international, randomised, multicentre, placebo-controlled, phase 3 trial. Lancet. 2014;383:31–9. doi:10.1016/S0140-6736(13)61719-5.

- Nowak RP, et al. Advances and challenges in understanding histone demethylase biology. Curr Opin Chem Biol. 2016;33:151–9. doi:10.1016/j.cbpa.2016.06.021.
- Hojfeldt JW, Agger K, Helin K. Histone lysine demethylases as targets for anticancer therapy. Nat Rev Drug Discov. 2013;12:917–30. doi:10.1038/nrd4154.
- Kooistra SM, Helin K. Molecular mechanisms and potential functions of histone demethylases. Nat Rev Mol Cell Biol. 2012;13:297–311. doi:10.1038/nrm3327.
- Xhabija B, Kidder BL. KDM5B is a master regulator of the H3K4-methylome in stem cells, development and cancer. Sem Cancer Biol. 2019;57:79–85. doi:10.1016/j.semcancer.2018.11.001.
- Yu X, et al. Chromatin remodeling: demethylating H3K4me3 of type I IFNs gene by Rbp2 through interacting with Piasy for transcriptional attenuation. FASEB journal: official publication of the Federation of American Societies for Experimental Biology. 2018;32:552–67. doi:10.1096/fj.201700088RR.
- Xu J, et al. Metabolic enzyme PDK3 forms a positive feedback loop with transcription factor HSF1 to drive chemoresistance. Theranostics. 2019;9:2999–3013. doi:10.7150/thno.31301.
- Zhou Q, et al. Inhibiting neddylation modification alters mitochondrial morphology and reprograms energy metabolism in cancer cells. JCI Insight 4, doi:10.1172/jci.insight.121582 (2019).
- Barysch SV, Dittner C, Flotho A, Becker J, Melchior F. Identification and analysis of endogenous SUMO1 and SUMO2/3 targets in mammalian cells and tissues using monoclonal antibodies. Nat Protoc. 2014;9:896–909. doi:10.1038/nprot.2014.053.
- Harris AL. Hypoxia–a key regulatory factor in tumour growth. Nat Rev Cancer. 2002;2:38–47. doi:10.1038/nrc704.
- Buuh ZY, Lyu Z, Wang RE. Interrogating the Roles of Post-Translational Modifications of Non-Histone Proteins. J Med Chem. 2018;61:3239–52. doi:10.1021/acs.jmedchem.6b01817.
- Kim YS, Keyser SG, Schneekloth JS. Jr. Synthesis of 2',3',4'-trihydroxyflavone (2-D08), an inhibitor of protein sumoylation. Bioorg Med Chem Lett. 2014;24:1094–7. doi:10.1016/j.bmcl.2014.01.010.
- Langston SP, et al. Discovery of TAK-981, a First-in-Class Inhibitor of SUMO-Activating Enzyme for the Treatment of Cancer. J Med Chem. 2021;64:2501–20. doi:10.1021/acs.jmedchem.0c01491.
- Yuan H, et al. Small ubiquitin-related modifier paralogs are indispensable but functionally redundant during early development of zebrafish. Cell Res. 2010;20:185–96. doi:10.1038/cr.2009.101.
- Rabellino A, Andreani C, Scaglioni PP. The Role of PIAS SUMO E3-Ligases in Cancer. Cancer research. 2017;77:1542–7. doi:10.1158/0008-5472.CAN-16-2958.
- Xu W, et al. KDM5B demethylates H3K4 to recruit XRCC1 and promote chemoresistance. Int J Biol Sci. 2018;14:1122–32. doi:10.7150/ijbs.25881.
- Hendriks IA, et al. Site-specific characterization of endogenous SUMOylation across species and organs. Nature communications. 2018;9:2456. doi:10.1038/s41467-018-04957-4.
- Cai Q, Verma SC, Kumar P, Ma M, Robertson ES. Hypoxia inactivates the VHL tumor suppressor through PIASy-mediated SUMO modification. PloS one. 2010;5:e9720. doi:10.1371/journal.pone.0009720.

- Chien W, et al. PIAS4 is an activator of hypoxia signalling via VHL suppression during growth of pancreatic cancer cells. Br J Cancer. 2013;109:1795–804. doi:10.1038/bjc.2013.531.
- Xu R, et al. Results of a randomized and controlled clinical trial evaluating the efficacy and safety of combination therapy with Endostar and S-1 combined with oxaliplatin in advanced gastric cancer. Onco Targets Ther. 2013;6:925–9. doi:10.2147/OTT.S46487.
- Eder JP Jr, et al. Phase I clinical trial of recombinant human endostatin administered as a short intravenous infusion repeated daily. J Clin Oncol. 2002;20:3772–84. doi:10.1200/JCO.2002.02.082.
- Wouters BG, Koritzinsky M. Hypoxia signalling through mTOR and the unfolded protein response in cancer. Nat Rev Cancer. 2008;8:851–64. doi:10.1038/nrc2501.
- Batie M, et al. Hypoxia induces rapid changes to histone methylation and reprograms chromatin. Science. 2019;363:1222–6. doi:10.1126/science.aau5870.
- Chakraborty AA, et al. Histone demethylase KDM6A directly senses oxygen to control chromatin and cell fate. Science. 2019;363:1217–22. doi:10.1126/science.aaw1026.
- Thienpont B, et al. Tumour hypoxia causes DNA hypermethylation by reducing TET activity. Nature. 2016;537:63–8. doi:10.1038/nature19081.
- Kim Y, et al. Methylation-dependent regulation of HIF-1alpha stability restricts retinal and tumour angiogenesis. Nature communications. 2016;7:10347. doi:10.1038/ncomms10347.
- Lee JY, et al. LSD1 demethylates HIF1alpha to inhibit hydroxylation and ubiquitin-mediated degradation in tumor angiogenesis. Oncogene. 2017;36:5512–21. doi:10.1038/onc.2017.158.
- Wilson VG. Introduction to Sumoylation. Adv Exp Med Biol. 2017;963:1–12. doi:10.1007/978-3-319-50044-7_1.
- Li J, et al. Cbx4 governs HIF-1alpha to potentiate angiogenesis of hepatocellular carcinoma by its SUMO E3 ligase activity. Cancer cell. 2014;25:118–31. doi:10.1016/j.ccr.2013.12.008.
- Carbia-Nagashima A, et al. RSUME, a small RWD-containing protein, enhances SUMO conjugation and stabilizes HIF-1alpha during hypoxia. Cell. 2007;131:309–23. doi:10.1016/j.cell.2007.07.044.
- Cheng J, Kang X, Zhang S, Yeh ET. SUMO-specific protease 1 is essential for stabilization of HIF1alpha during hypoxia. Cell. 2007;131:584–95. doi:10.1016/j.cell.2007.08.045.
- Desterro JM, Rodriguez MS, Hay RT. SUMO-1 modification of IkappaBalpha inhibits NF-kappaB activation. Molecular cell. 1998;2:233–9. doi:10.1016/s1097-2765(00)80133-1.
- Guzzo CM, et al. RNF4-dependent hybrid SUMO-ubiquitin chains are signals for RAP80 and thereby mediate the recruitment of BRCA1 to sites of DNA damage. Sci Signal. 2012;5:ra88. doi:10.1126/scisignal.2003485.
- Raimondi A, et al. Genomic markers of resistance to targeted treatments in gastric cancer: potential new treatment strategies. Pharmacogenomics. 2018;19:1047–68. doi:10.2217/pgs-2018-0077.
- Fu YD, et al. Targeting histone demethylase KDM5B for cancer treatment. Eur J Med Chem. 2020;208:112760. doi:10.1016/j.ejmech.2020.112760.

- Zheng YC, et al. Lysine demethylase 5B (KDM5B): A potential anti-cancer drug target. Eur J Med Chem. 2019;161:131–40. doi:10.1016/j.ejmech.2018.10.040.
- Sachdev S, et al. PIASy, a nuclear matrix-associated SUMO E3 ligase, represses LEF1 activity by sequestration into nuclear bodies. Genes Dev. 2001;15:3088–103. doi:10.1101/gad.944801.
- Gross M, Yang R, Top I, Gasper C, Shuai K. PIASy-mediated repression of the androgen receptor is independent of sumoylation. Oncogene. 2004;23:3059–66. doi:10.1038/sj.onc.1207443.

Figures

Fig. 1

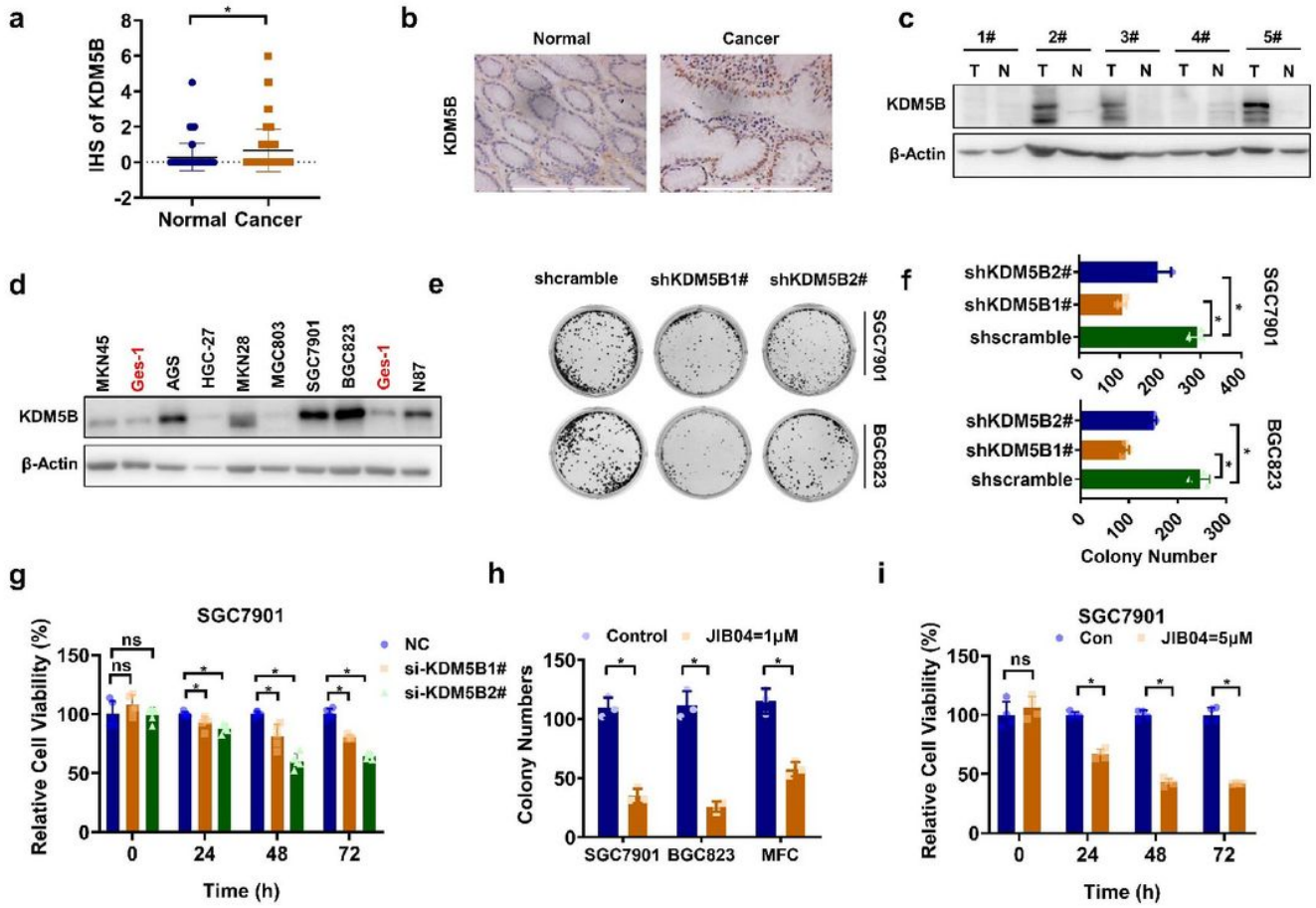

Figure 1

KDM5B was upregulated to promote cell proliferation in GC a Immunohistochemical staining of KDM5B in tissue microarray containing 77 GC tissue and corresponding adjacent normal tissues. The H-score was calculated and analyzed. (n=77, Student's t-test, *p<0.05). b Represented photos of KDM5B IHC in GC tissue and normal tissue. c Expression of KDM5B protein in fresh GC tissue and adjacent normal tissue was analyzed by Western blotting. d Expression of KDM5B protein in GC cell lines and GES-1 cell line was

analyzed by Western blotting. e Plate colony formation assay for SGC7901 and BGC823 cells transfected with shKDM5B or scramble control (shscramble) containing lentiviral particles. f The number of colonies with more than 50 cells was counted and quantified (mean ± SD, n = 3, one-way ANOVA, *p<0.05). g Relative cell viability of SGC7901 cells at 24h, 48h and 72h after transient transfection with KDM5B or negative control (NC) siRNA was measured with CCK8 assay (mean ± SD, n = 3, one-way ANOVA, *p<0.05). h SGC7901, BGC823 and MFC cells were treated with JIB04 (1μM) and colony formation was analyzed (mean ± SD, n = 3, one-way ANOVA, *p<0.05). i Relative cell viability of SGC7901 cells at 24h, 48h and 72h after treatment of JIB04 (5μM) was determined with CCK8 assay (mean ± SD, n = 3, one-way ANOVA, *p<0.05).

Fig. 2

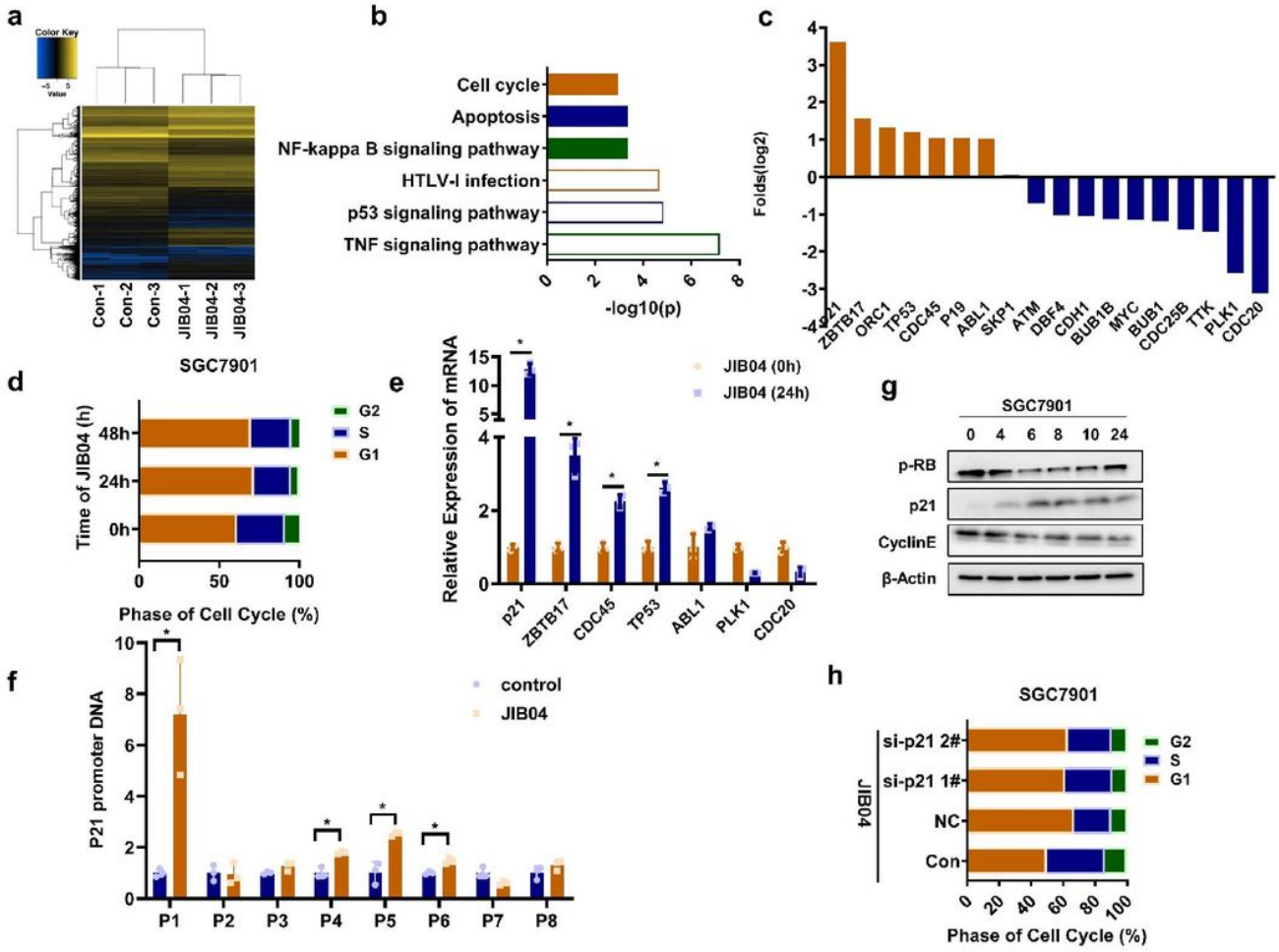

Figure 2

KDM5B repressed p21 transcription to induce cell cycle arrest at G1 Cluster analysis (a) and KEGG analysis (b) of the mRNA profile on JIB-04-treated GC cells. c Flow cytometry analysis of cell cycle inSGC7901 cells before and after treatment of JIB04 (5μM) at 24 and 48 hours. d Significantly differentially expressed genes involved in cell cycle regulation. e qPCR was performed to verify the result of sequencing. f The binding of tri-methylation H3K4 to p21 promoter in SGC7901 cells before and after JIB04 treatment was assessed by ChIP assay. g The expression of G1 phase regulatory proteins in

SGC7901 cells treated with JIB04 (5μM) for various times were evaluated by Western blotting. h Flow cytometry analysis of cell cycle in SGC7901 cells with the treatment as indicated.

Fig. 3

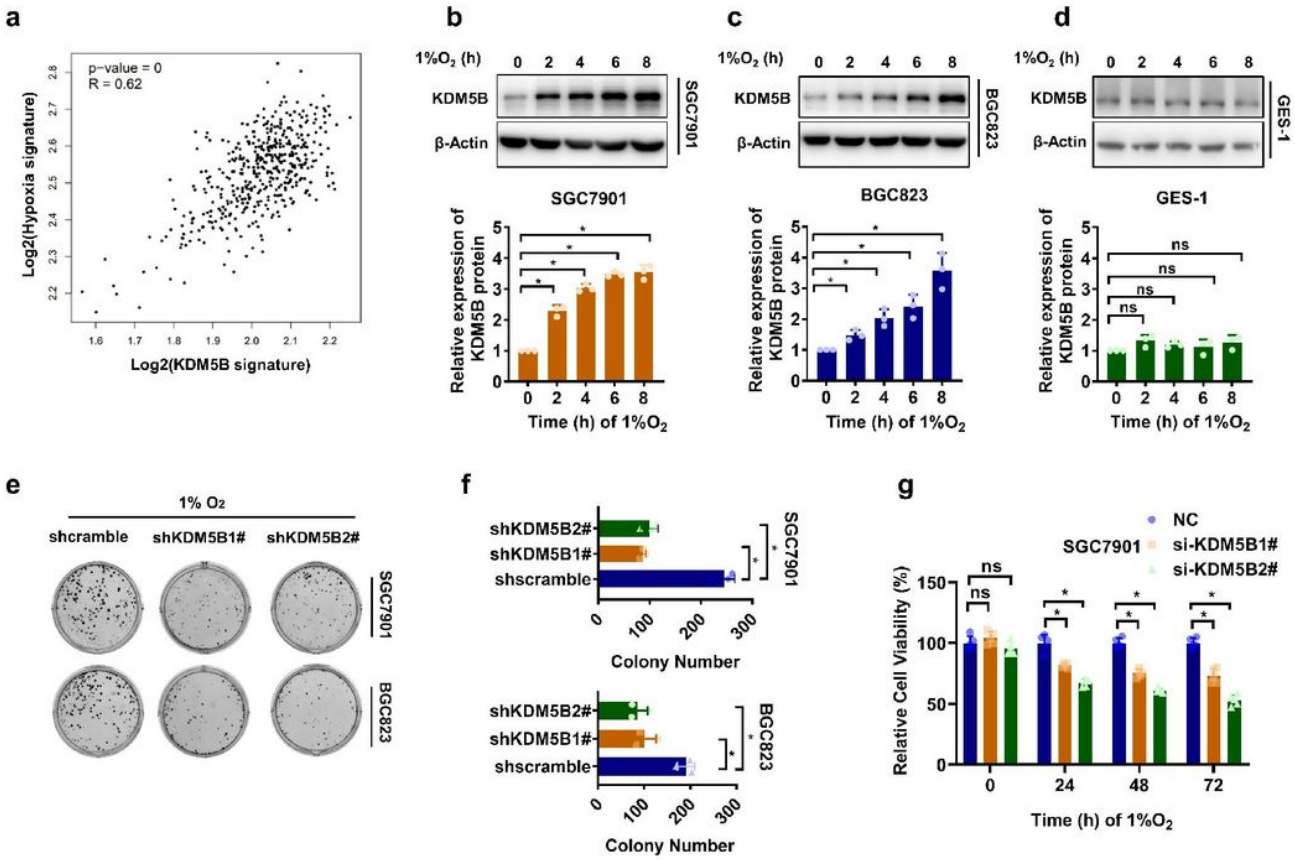

Figure 3

KDM5B protein was upregulated to facilitate hypoxia adaption a The correlation of 1,267 putative KDM5B-dependent genes and hypoxia signature was detected by GEPIA. b-d KDM5B protein expression in SGC7901 (b), BGC823 (c), GES-1 (d) cells cultured under hypoxia (1%O2) was determined by Western blotting (upper panel). The relative KDM5B protein expression was calculated from 3 individual experiments after scanning the blot with ImageJ software (down panel). e, d Plate colony formation assay for SGC7901 and BGC823 cells before and after KDM5B-knock-down were evaluated under hypoxia condition (1%O2) (mean ± SD, n = 3, one-way ANOVA, *p<0.05). g CCK8 assay was applied to measure the relative viability of SGC7901 cells under hypoxia condition (1%O2) at 24h, 48h and 72h after KDM5B knock-down (mean ± SD, n = 3, one-way ANOVA, *p<0.05).

Fig. 4

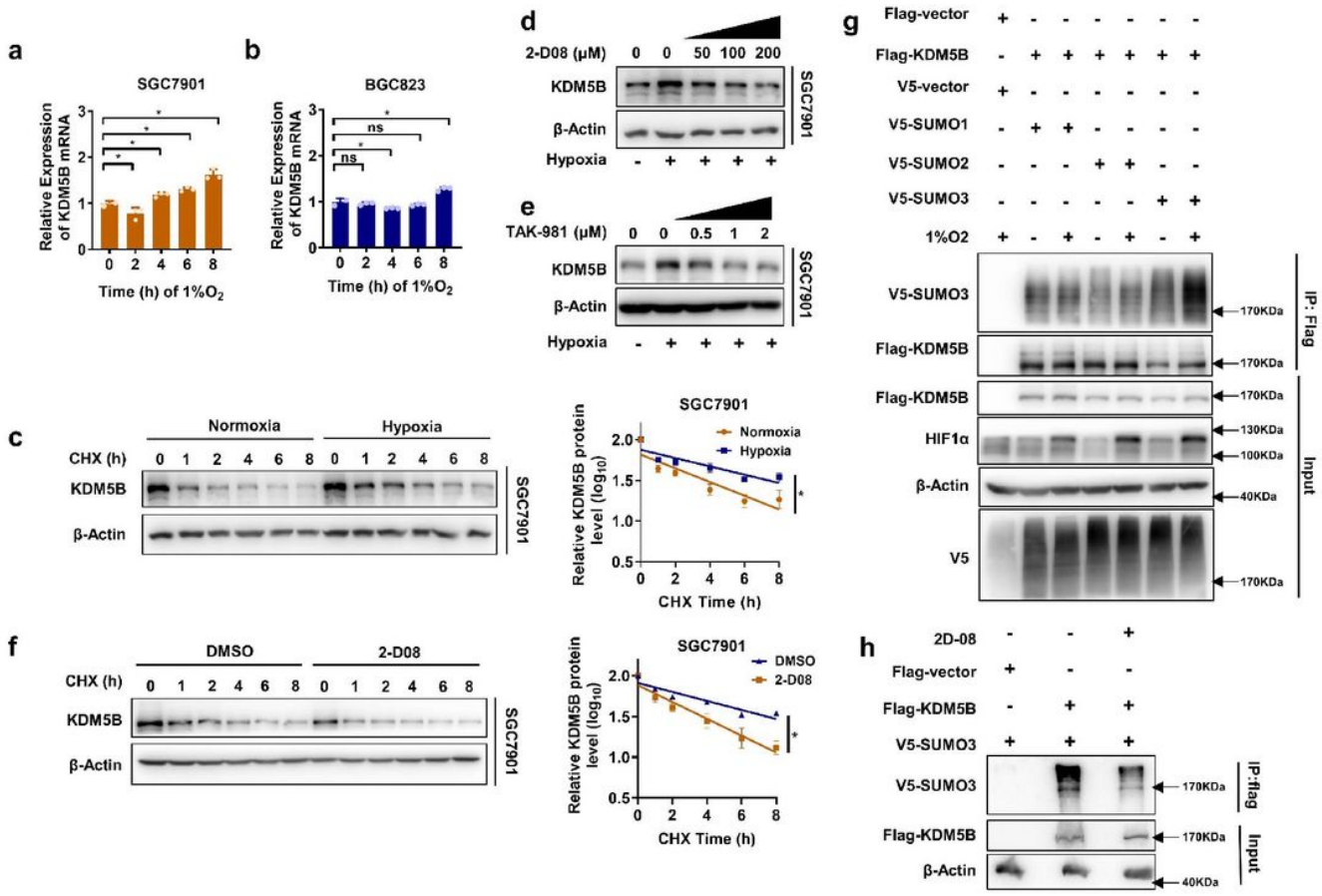

Figure 4

Hypoxia induced SUMO3-dependent SUMOylation and subsequent stabilization of KDM5B a, b qPCR analysis of KDM5B mRNA expression in SGC7901 (a) and BGC823 (b) cells at indicated time points under hypoxia (1%O2) (mean ± SD, n = 3, one-way ANOVA, *p<0.05). c The half-life of KDM5B protein in SGC7901 cells under normoxia and hypoxia condition (1%O2) was determined by CHX assay. The relative KDM5B protein expression was measured by ImageJ, and Semi-log plot were shown on the right panel (mean ± SD, n = 3, ANCOVA analysis, *p<0.05). d, e KDM5B protein expression in SGC7901 cells treated with 2-D08 (d) or TAK-981 (e) as indicated was determined by Western blotting. f The half-life of KDM5B protein in SGC7901 cells under hypoxia (1%O2) with 2-D08 (200μM) or DMSO treatment was determined by CHX assay. The relative KDM5B protein expression was quantified by ImageJ (mean ± SD, n = 3, ANCOVA analysis, *p<0.05). g HEK293T cells co-transfected with indicated plasmids for 48h, and the SUMOylation assay was performed after 6h 1%O2 treatment. h HEK293T cells co-transfected with Flag-KDM5B and V5-SUMO3 for 48h before 2-D08（200μM）treatment for another 24h were subjected to SUMOylation assay.

Fig. 5

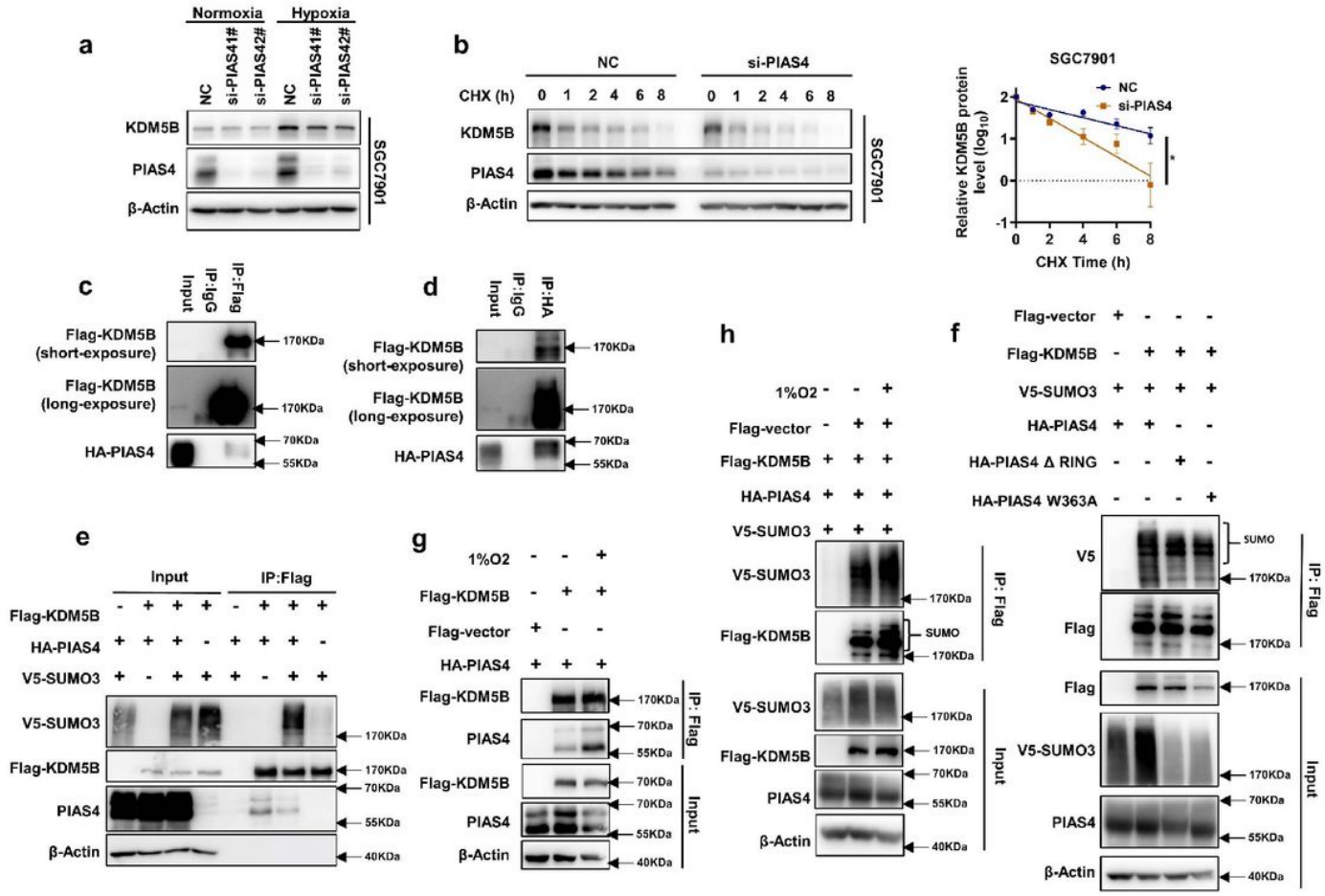

Figure 5

PIAS4 was the SUMO E3 ligase for hypoxia-induced KDM5B SUMOylation a The expression of KDM5B protein in SGC7901 cells under normoxia or 1%O2 with or without PIAS4 knockdown by siRNA was analyzed by Western blotting. b SGC7901 was transiently transfected with PIAS4 siRNA for 48h later with cycloheximide (CHX) and 1% O2 treatment for the indicated times, and then the half-life of KDM5B was analyzed by Western blotting and followed with measurement by ImageJ and the p-value derived from ANCOVA analysis comparing NC and si-PIAS4 (mean ± SD, n = 3, ANCOVA analysis, *p<0.05). c, d Co-IP was performed to detect the interaction between exogenous expression Flag-KDM5B and HA-PIAS4 in HEK293T. Respectively, the Flag (c) and HA (d) antibody (IgG was used as negative control) was used for immunoprecipitation and the other for western blotting analysis. e SUMOylation assay was employed to HEK293T co-transfected with indicated plasmids for 48h followed 6h 1% O2 treatment. The SUMOylation of KDM5B with or without exogenous expression of wild-type PIAS4 was determined by western blotting. f The SUMOylation analysis of KDM5B in HEK293T co-transfected with E3 activity inactivation mutant PIAS4 (HA-PIAS4 ΔRING 44, HA-PIAS4 W363A 45 and wild-type PIAS4 under hypoxia condition. g The interaction between exogenous Flag-KDM5B and HA-PIAS4 under hypoxia condition was determined by co-IP. h The SUMOylation of KDM5B under normoxia and hypoxia was analyzed as indicated by SUMOylation assay.

Fig. 6

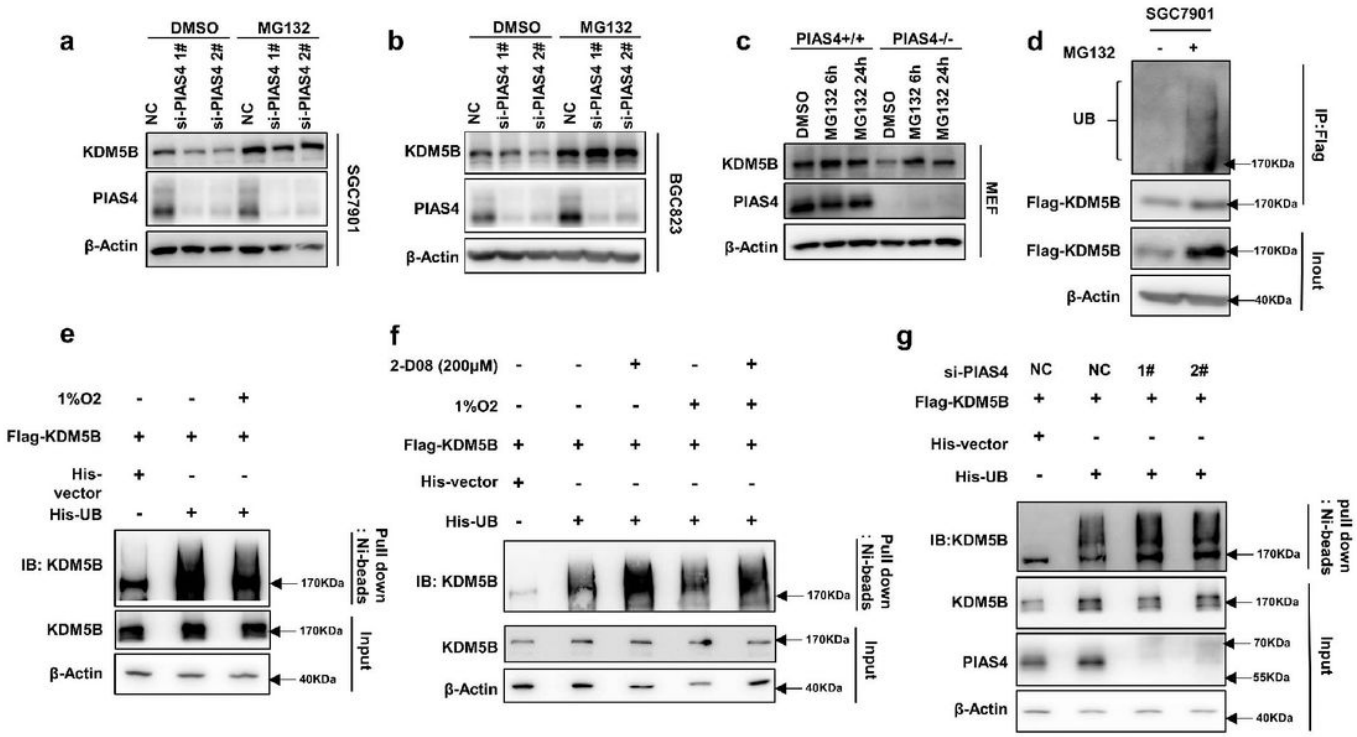

Figure 6

PIAS4-mediated KDM5B SUMOylation prevented it from ubiquitination-dependent proteasomal degradation a, b KDM5B protein level in SGC7901 (a) and BGC823 (b) cells treated with MG132 (20μM 6h) after PIAS4 knockdown were detected by western blotting. c KDM5B protein level in Pias4-/- and Pias4+/+ MEF cells after treatment of MG132 (20μM 6h, 5μM 24h) under 1% O2 were determined by western blotting. d SGC7901 was transfected with Flag-KDM5B for 48h and the proteins immunoprecipitated by Flag antibody were analyzed with western blotting. e Ni-beads Pull down assay was performed with HEK293T co-transfected Flag-KDM5B, His-UB or corresponding empty vector as indicated for 48h later with 1% O2 and MG132 (20μM) treatment for 6h. KDM5B antibody was used to detect ubiquitination KDM5B for western blotting. f HEK293T was co-transfected with indicated plasmids for 48h followed with 2-D08 (200μM) for 24h and 1% O2 and MG132 (20μM) for 6h before the Ni-beads pull-down assay was performed to determine the ubiquitination of KDM5B. g HEK293T was co-transfected with Flag-KDM5B, His-UB or corresponding empty vector as indicated and PIAS4 siRNA for 48h. After the treatment of 1%O2 and MG132 (20μM) for 6h, the Ni-beads pull-down assay was applied to analyze the ubiquitination of KDM5B.

Fig. 7

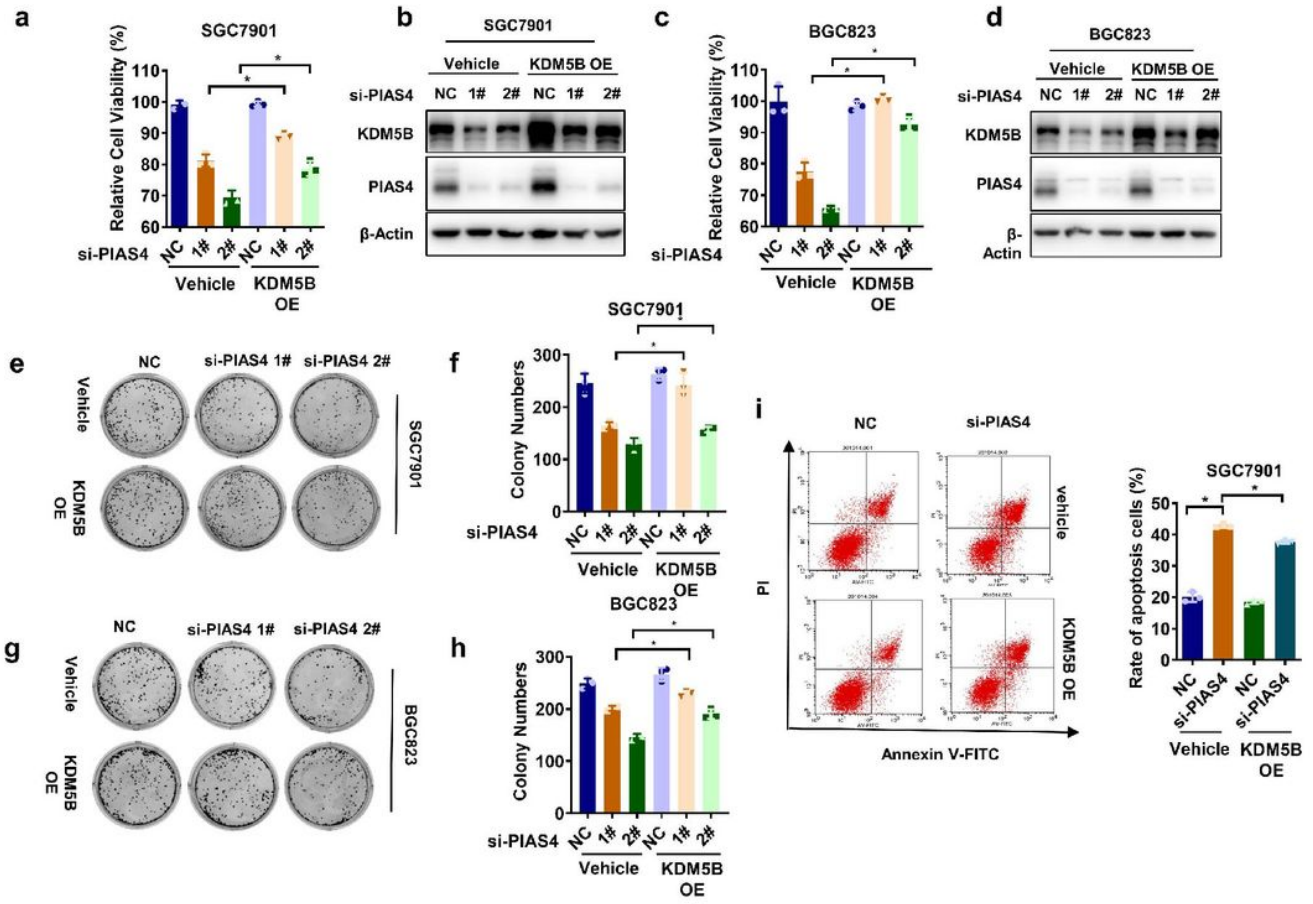

Figure 7

PIAS4 upregulated KDM5B to promote hypoxia adaption. a Relative cell viability of SGC7901 was determined by CCK8 assay after co- transfected with PIAS4 siRNA or NC siRNA and Flag-KDM5B or corresponding empty vector as indicated for 72h under 1%O2 condition. NC group was normalized respectively in vehicle and KDM5B OE group (mean ± SD, n = 3, one-way ANOVA, *p<0.05). b The expression of KDM5B was detected in SGC7901 cells after co-transfected with PIAS4 siRNA or NC siRNA and Flag-KDM5B or corresponding empty vector as indicted under 1%O2 condition by western blotting. c Relative cell viability of BGC823 cells was determined by CCK8 assay as described in (a). d The expression of KDM5B was detected in BGC823 cells as described in (b). e SGC7901 cells was co-transfected with PIAS4 siRNA or NC siRNA and Flag-KDM5B or corresponding empty vector as indicted for 24h before replating as single cell suspensions for colony formation for 10 days under 1%O2 condition. f The number of colonies in (e) with more than 50 cells was counted and quantified (mean ± SD, n = 3, one-way ANOVA, *p<0.05). g Colony formation assay was performed as described in (e) in BGC823 cells. h The number of colonies in (g) with more than 50 cells was counted and quantified (mean ± SD, n = 3, one-way ANOVA, *p<0.05). i SGC7901 cells were co-transfected with PIAS4 siRNA or NC siRNA and Flag-KDM5B or corresponding empty vector as indicated for 24h followed with 1%O2 treatment for 24h before cells were collected for Flow cytometry analysis of cell apoptosis.

Fig. 8

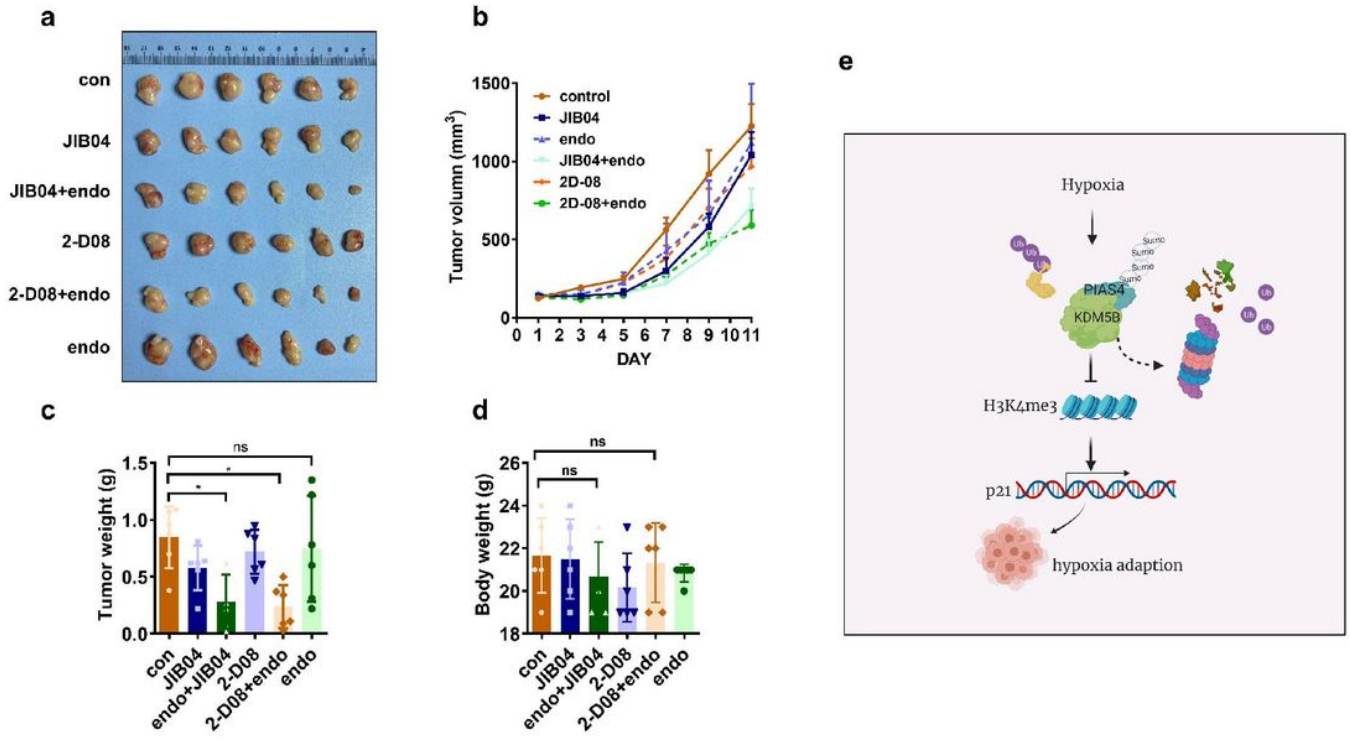

Figure 8

Targeting KDM5B to overcome hypoxia adaption in vivo a-d MFC cells were subcutaneously injected into the flanks of nude mice to generate Xenograft tumors (n=6). And were treated as indicated to evaluate the effect of JIB04, Endostar and 2-D08 on tumorigenicity. The representative image (a), Tumor Growth Curve (b), the tumor weight of xenograft at sacrifice (c), and the body weight of mice at sacrifice (d) after 11 DAYs drug injection. e A schematic illustration of the model depicting the PIAS4-mediated SUMOylation protected KDM5B from ubiquitination-dependent proteasomal degradation of KDM5B to promote hypoxia adaption of gastric cancer.

Supplementary Files

This is a list of supplementary files associated with this preprint. Click to download.

- Additionalfile.docx